RESEARCH ARTICLE

CELL BIOLOGY

Light-regulated collective contractility in a multicellular choanoflagellate

Thibaut Brunet[1]*, Ben T. Larson[1,2]*, Tess A. Linden[1]*, Mark J. A. Vermeij[3], Kent McDonald[4], Nicole King[1]†

Collective cell contractions that generate global tissue deformations are a signature feature of animal movement and morphogenesis. However, the origin of collective contractility in animals remains unclear. While surveying the Caribbean island of Curaçao for choanoflagellates, the closest living relatives of animals, we isolated a previously undescribed species (here named *Choanoeca flexa* sp. nov.) that forms multicellular cup-shaped colonies. The colonies rapidly invert their curvature in response to changing light levels, which they detect through a rhodopsin–cyclic guanosine monophosphate pathway. Inversion requires actomyosin-mediated apical contractility and allows alternation between feeding and swimming behavior. *C. flexa* thus rapidly converts sensory inputs directly into multicellular contractions. These findings may inform reconstructions of hypothesized animal ancestors that existed before the evolution of specialized sensory and contractile cells.

The evolution of animals from their single-celled ancestors involved several major evolutionary innovations, including multicellularity, spatial cell differentiation, and morphogenesis (*1*, *2*). Efforts to reconstruct the origin of animal multicellularity have benefited from the study of choanoflagellates, the closest living relatives of animals (*3*–*5*). Choanoflagellates are microbial eukaryotes that feed on bacteria and live in aquatic environments around the world; many species differentiate over their life history into diverse cell types, including unicellular and multicellular forms (*3*, *6*–*8*). Comparative genomics has revealed many gene families once thought to be unique to animals (such as cadherins, C-type lectins, and receptor tyrosine kinases) in choanoflagellates (*4*, *9*–*12*). Moreover, the model choanoflagellate *Salpingoeca rosetta* (*6*) exhibits diverse responses to environmental cues, including pH-taxis (*13*), aerotaxis (*14*), and bacterial regulation of multicellular development (*15*) and mating (*16*). However, *S. rosetta* is only one of ~380 known species (*17*), and choanoflagellates are at least as genetically diverse as animals (*9*). Choanoflagellate diversity thus represents a largely untapped opportunity to investigate environmental regulation of cell behavior, the principles that broadly underpin multicellularity, and the evolution of animal cell biology. We report here on the discovery of light-regulated collective cell contractility in a recently isolated multicellular choanoflagellate. This finding reveals that apical cell contractility evolved before the origin of animal multicellularity.

[1]Howard Hughes Medical Institute and the Department of Molecular and Cell Biology, University of California, Berkeley, CA, USA. [2]Biophysics Graduate Group, University of California, Berkeley, CA, USA. [3]Department of Aquatic Microbiology, Institute for Biodiversity and Ecosystem Dynamics, University of Amsterdam, CARMABI, Piscaderabaai z/n Willemstad, Curaçao. [4]Electron Microscopy Laboratory, University of California, Berkeley, CA, USA.
*These authors contributed equally to this work.
†Corresponding author. Email: nking@berkeley.edu

Photic cues induce sheet inversion in a colonial choanoflagellate

During a survey of choanoflagellate diversity on the Caribbean island of Curaçao (Fig. 1, A and B), we collected large, cup-shaped colonies of protozoa (~100 μm in diameter) from shallow splash pools above the tide line of a rocky coastal area (Fig. 1B). Each colony was composed of a monolayer ("sheet") of up to hundreds of flagellated cells (Fig. 1C and movie S1). The cells bore the characteristic collar complex of choanoflagellates (*1*, *3*), in which a "collar" of microvilli surrounds a single apical flagellum (Fig. 1D). However, unlike in most choanoflagellate colonies (*3*), the apical flagella pointed into the interior of the colony (Fig. 1E), resembling the orientation of collar cells in the choanocyte chambers of sponges (*18*). The colonies inverted rapidly (within ~30 s from initiation to completion) while maintaining their cell topology, such that the flagella pointed outward along the radius of curvature of the colony (Fig. 1, F and G, and movie S2). The colonies tended to remain in the inverted form ("flagella-out") for several minutes before reverting to their initial, relaxed conformation ("flagella-in") in a similarly rapid process (Fig. 1H and movie S3).

To start laboratory cultures of this choanoflagellate, we manually isolated representative colonies away from the other microbial eukaryotes in the splash pool sample (for example, presumptive *Oxyrrhis* sp. dinoflagellates) (Fig. 1C and movie S1) and transferred them into nutrient-supplemented artificial seawater along with co-isolated environmental bacteria (which choanoflagellates need as a food source). Analysis of the 18*S* ribosomal DNA (rDNA) sequence indicated that the choanoflagellate is the sister species of the previously described *Choanoeca perplexa* (also known as *Proterospongia choanojuncta*) (Fig. 1J and fig. S1), whose life history includes both single cells and colonies (*7*, *19*). Inspired by the sheet-bending behavior of the Curaçao choanoflagellate, we named it *Choanoeca flexa*. [A similar behavior was mentioned in a 1983 study of *C. perplexa* (*7*), but the culture subsequently stopped forming colonies, preventing further study (*3*).] *C. flexa* sheet inversion, representing a global change in multicellular form, is reminiscent of concerted movement and morphogenesis in animals (such as muscle contraction or gastrulation). Because of the potential evolutionary implications of rapid shape change in *C. flexa*, we investigated (i) how colony inversion is regulated, (ii) the mechanisms underlying colony inversion, and (iii) the ecological consequences of colony inversion.

Several lines of evidence indicated that light levels regulate *C. flexa* colony inversion. While imaging *C. flexa* sheets for >1 hour under constant illumination, colony inversions became less frequent. By contrast, after the microscope illumination was turned off, the colonies inverted almost immediately (movie S4). To quantify light-to-dark–induced *C. flexa* inversion, we established an assay based on the observation that the projected area of a *C. flexa* sheet decreases by as much as 50% during inversion (Fig. 2, A to C, and movie S5). Using this assay, we confirmed that a rapid decrease in illumination reliably induces inversion of *C. flexa* colonies within 30 s (Fig. 2D and movie S6). Choanoflagellates had previously been thought to be insensitive to light (*20*).

A rhodopsin-cGMP pathway regulates colony inversion in response to light-to-dark transitions

We next investigated how *C. flexa* colonies sense and respond to changing light levels. Although choanoflagellates are unpigmented and transparent, at least four species encode a choanoflagellate-specific rhodopsin-phosphodiesterase fusion protein (fig. S2) (*9*), RhoPDE, that has been investigated as a potential optogenetic tool (*21*–*24*). RhoPDEs consist of an N-terminal type I rhodopsin [a photosensitive transmembrane protein broadly involved in light detection (*25*)] fused to a C-terminal phosphodiesterase (PDE) that catalyzes cyclic nucleotide hydrolysis (Fig. 3A). In in vitro studies (*21*–*24*), *S. rosetta* RhoPDE appears capable of converting a photic stimulus into a biochemical signal within seconds, similar to the time scale of the *C. flexa* response to light-to-dark transitions.

To search for RhoPDE or other candidate photosensitive proteins in *C. flexa*, we sequenced and assembled the *C. flexa* transcriptome (*26*), which we found to encode four RhoPDE homologs (fig. S2) (GenBank accession numbers MN013138, MN013139, MN013140, and MN013141). No other rhodopsins were detected in the *C. flexa* transcriptome. The only other candidate photoreceptor protein domain found was a cryptochrome transcription factor (*27*), which is predicted to act on the time scale of transcriptional regulation [at least several minutes (*28*, *29*)] and, therefore, is unlikely to mediate the light-to-dark transition response. Thus, we focused our attention on the RhoPDEs.

If RhoPDE regulates the light-to-dark transition response, depletion of the rhodopsin chromophore, retinal (*30*, *31*), should abolish rhodopsin activity and thereby prevent the response. Moreover, artificially increasing the cellular concentration of cyclic guanosine monophosphate (cGMP) or cyclic adenosine monophosphate (cAMP) (which are degraded by the enzymatic activity of PDEs) should mimic the effect of darkness and be sufficient to trigger sheet inversion.

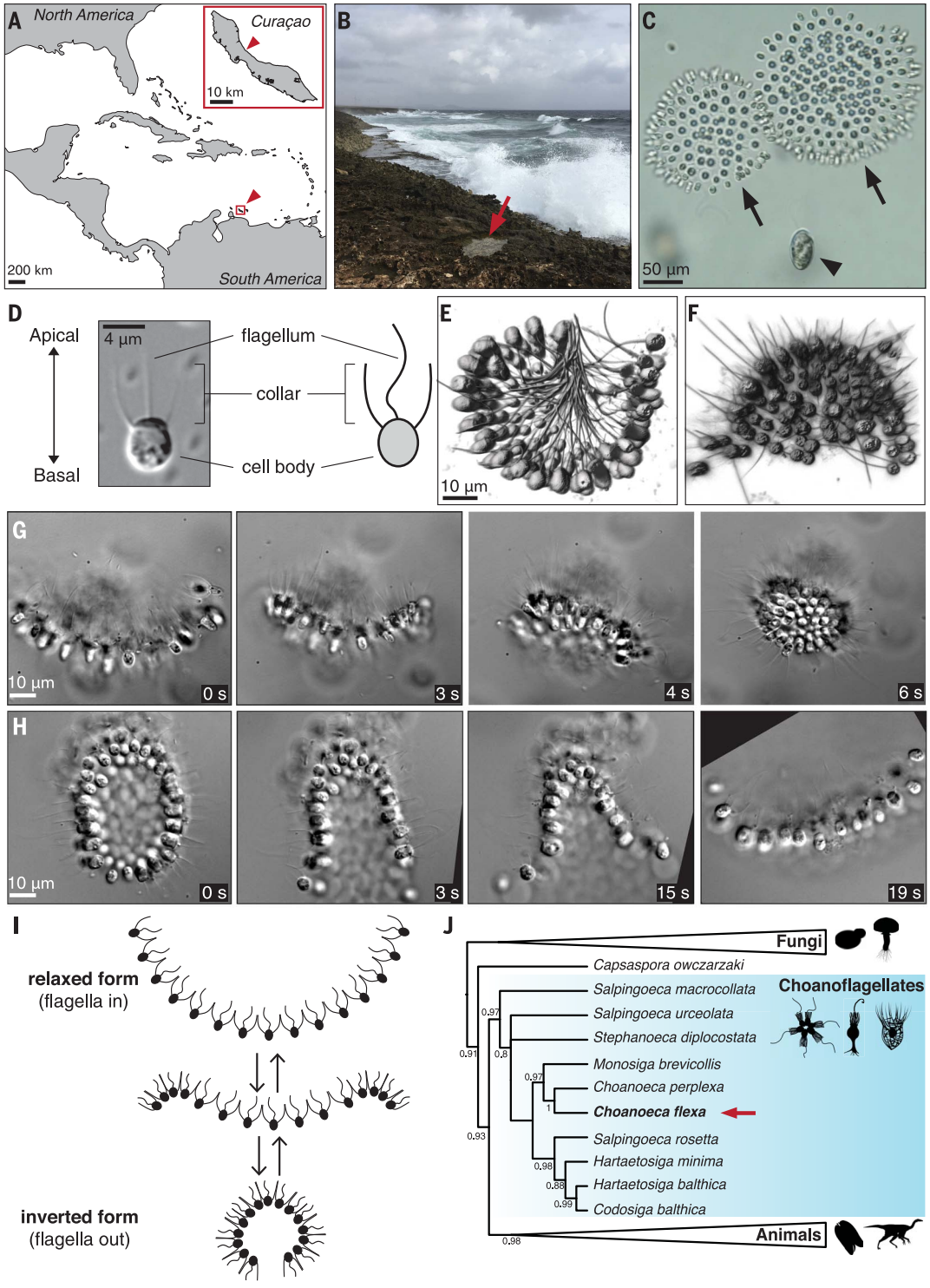

Fig. 1. Multicellular sheets of a colonial choanoflagellate from Curaçao rapidly and reversibly invert in curvature. (**A** to **C**) *C. flexa* was isolated from splash pools on the northern shore of Curaçao. (A) Map of the Caribbean Sea. Arrowhead: Curaçao. (Inset) Map of Curaçao. Inset arrowhead: sampling site (12°13′38.9″ N 69°00′47.0″ W). (B) Photograph of the sampling site. Arrow: splash pool. (C) Microscopy of freshly collected splash pool sample revealed a diverse microeukaryotic community, including dinoflagellates (*Oxyrrhis* sp.; arrowhead) and cup-shaped choanoflagellate colonies (*C. flexa*; arrows) that rapidly inverted their curvature. Still frame from movie S1. (**D**) Diagnostic features of choanoflagellate cell morphology shown by differential interference contrast (DIC) micrograph and sketch of a *C. flexa* cell. (**E** and **F**) *C. flexa* colonies alternate between two conformations, flagella-in (E) and flagella-out (F). (**G** and **H**) *C. flexa* colonies rapidly and reversibly invert their curvature while maintaining contacts among neighboring cells. (G) Flagella-in colony inverts to the flagella-out orientation (movie S2). (H) Flagella-out colony reverts to the flagella-in orientation (movie S3). Movie frames were rotated to facilitate tracking individual cells between images. (**I**) Summary of the inversion and relaxation processes. (**J**) Phylogenetic analysis of 18*S* rDNA sequences revealed that *C. flexa* (bold) is a sister to the choanoflagellate *C. perplexa* (*19*). (Scaled branch lengths are in Fig. S1.)

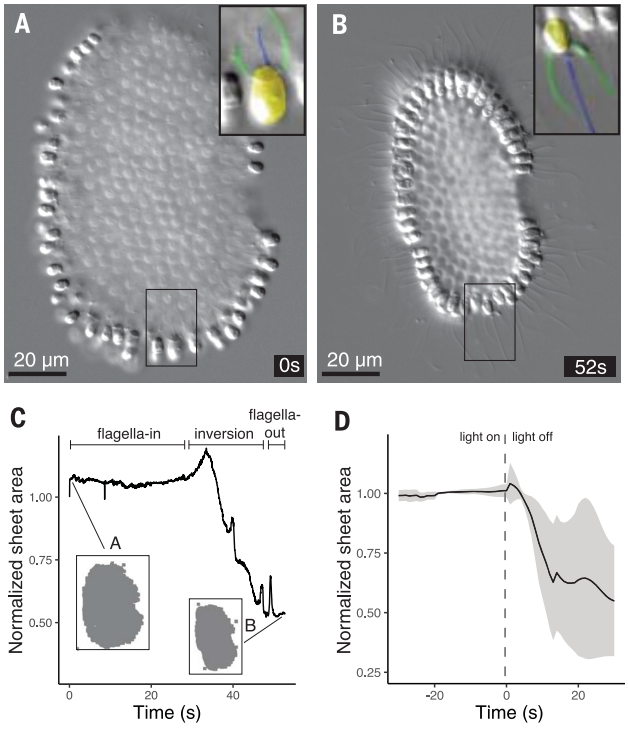

Fig. 2. Light-to-dark transitions induce C. flexa colony inversion. (**A** to **C**) Colony inversion correlates with a decrease in the projected area of the colony. (A and B) *C. flexa* colony spontaneously inverts from the flagella-in (A) to the flagella-out (B) orientation (movie S5). (Insets) Pseudocoloring highlights the orientations of the cells in the boxed regions. Cell orientation relative to colony curvature inverts without breaking contacts with neighboring cells. (C) The projected area of the colony from (A) and (B) decreased by ~50% during inversion. Sheet area was normalized to its preinversion projected area. (**D**) Colonies reliably undergo inversion in response to light-to-dark transitions. Normalized projected area of $n = 5$ colonies over time before and after light reduction (vertical dashed line). Line: mean projected area (rolling average over 5-s windows); ribbon: standard deviation.

Plants and some bacteria synthesize retinal and other carotenoids, but the *C. flexa* transcriptome lacks a key enzyme in the retinal biosynthesis pathway (fig. S3). Therefore, like animals, *C. flexa* must receive retinal or its precursor, beta-carotene, from its food. It is possible that *C. flexa* acquires retinal or beta-carotene from its bacterial prey, with which it is cultured. To test whether bacterially produced carotenoids are required for light-regulated colony inversion, we established a culture containing only *C. flexa* and a co-isolated bacterium, *Pseudomonas oceani*, that lacks genes in the retinal biosynthesis pathway (fig. S3) (*32*). This culture, named "ChoPs" (for *Choanoeca* + *Pseudomonas*), was expected to be devoid of carotenoids, thereby abolishing rhodopsin activity. As predicted, *C. flexa* sheets in ChoPs cultures did not invert in response to darkness (Fig. 3B). Inoculating ChoPs cultures with a mixture of co-isolated environmental bacteria restored the light-to-dark response, demonstrating that a bacterial factor is necessary for the response. Addition of exogenous retinal to ChoPs cultures restored the wild-type light-to-dark response (Fig. 3C), indicating that the absence of retinal explains the absence of colony inversion. The requirement of retinal for the inversion response and the fact that all rhodopsin-encoding genes in the *C. flexa* are RhoPDEs suggest that one (or more) RhoPDE mediates the light-to-dark–induced inversion.

We next investigated whether cyclic nucleotide signaling influences *C. flexa* inversion. Treatment of *C. flexa* sheets with two inhibitors of PDE activity, caffeine (*33*) and 3-isobutyl-1-methylxanthine (IBMX) (*34*), induced colony inversion in the absence of a photic stimulus (Fig. 3D). Moreover, incubating *C. flexa* sheets with a cell-permeant analog of cGMP induced colony inversion in a dose-responsive manner, whereas a cell-permeant analog of cAMP had no effect (Fig. 3E), suggesting that cGMP acts as a second messenger in phototransduction and thereby triggers colony inversion.

Together, these results indicate that the *C. flexa* response to light-to-dark transitions relies on a rhodopsin as a photoreceptor and cGMP as a second messenger. The simplest interpretation of these findings is that a RhoPDE controls *C. flexa* phototransduction. However, direct validation will require targeted disruption of all four *C. flexa* RhoPDE homologs (fig. S2).

Sheet inversion mediates a trade-off between feeding and swimming

What are the functional and ecological roles of sheet inversion in *C. flexa*? Flagella-in sheets showed little to no motility, either slowly drifting or settling to the bottom of flasks (movie S7), whereas inverted (flagella-out) sheets swam rapidly (Fig. 4, A and B; fig. S5; and movie S4). By contrast, cells in flagella-in sheets fed efficiently (>75% cells per sheet internalizing beads), whereas cells in flagella-out sheets did not (~10% cells per sheet internalizing beads on average) (Fig. 4, C to G). Moreover, in relaxed sheets, fluid flow converged toward the center of the colony (carrying bacterial prey toward the cells), whereas in inverted sheets, the flow was directed away from the colony, allowing swimming but not feeding (fig. S6). Thus, sheet inversion increases motility, which may allow escape from environmental hazards (including predators), whereas sheet relaxation allows enhanced feeding efficiency.

Because sheets swim slowly when relaxed and rapidly when inverted, we suspected that darkness-induced inversion might allow sheets to accumulate in bright areas, effectively undergoing phototaxis. Using chambers illuminated with directional light, we found that *C. flexa* sheets tended to accumulate near the illumination source compared with a control in which no illumination was provided (Fig. 4H and fig. S7). Further, neither sheets from ChoPs cultures nor single cells from dissociated sheets were capable of phototaxis, suggesting that rhodopsin activity, multicellularity, and sheet inversion are all required for phototaxis (Fig. 4H). Thus, sheet inversion mediates an ecologically relevant trade-off between feeding and swimming (Fig. 4I).

Sheet inversion requires apical actomyosin contractility

How do cells in sheets interact, and what mechanisms allow sheet inversion? We found that cells in *C. flexa* sheets form direct contacts between their collar microvilli (Fig. 5, A to C, and fig. S8) but not through the intercellular bridges, shared extracellular matrix, or filopodial contacts that mediate multicellularity in other choanoflagellate species (*6*, *7*, *10*, *35*). Collar morphology differs between relaxed and inverted sheets. In relaxed sheets (flagella-in; Fig. 5C), the microvilli on each cell assemble into a barrel-shaped collar whose diameter varied little from base to tip. In inverted sheets (flagella-out; Fig. 5C), the microvilli form a flared, cone-shaped collar whose diameter increases from base to tip. Active "opening out" of the collar, by increasing

the surface area of the apical side of the sheets relative to their basal side, might force a change in sheet curvature. Consistent with this, the collar of dissociated *C. flexa* cells treated with caffeine opened into a conical shape, straightened, and slid down toward the base of the cell, whereas untreated controls maintained a barrel-shaped collar (Fig. 5, D to G, and fig. S9). These data suggest that the changes in collar geometry during inversion are actively generated by individual cells and do not require interactions among neighboring cells.

Sheet bending in animal epithelia is frequently mediated by apical constriction, in which contraction of an apical actomyosin network reduces the surface area of the apical side of the cell (*36*, *37*). Apical constriction is mediated by molecular motors belonging to the myosin II family, which predates the diversification of modern eukaryotes (*38*) and is found in all choanoflagellate genomes (*39*) and transcriptomes (*9*) published to date. *C. flexa* encodes homologs of the myosin II regulatory light chain (GenBank accession MK787241) and heavy chain (GenBank accession MK787240) (fig. S4), whose protein sequences are 78 and 63% similar, respectively, to their human counterparts.

In choanoflagellates and animal epithelial cells, the apical pole is defined by the presence of a flagellum or cilium, respectively, and/or microvilli, and the apicobasal axis of both types of cells is broadly considered to be homologous (*40*). *C. flexa* sheets contain a pronounced F-actin ring at the apical pole of each cell, from which the microvillar collar extends (Fig. 5H). Extending from this ring, we detected a small number of longitudinal actin fibers (usually two or three) pointing toward the basal pole. Diameter measurements showed that the F-actin ring was consistently smaller in inverted sheets compared with relaxed sheets (Fig. 5, I to L). The same was true for dissociated, caffeine-treated cells compared with the corresponding negative controls (Fig. 5, I to J and L), consistent with the ring actively constricting during sheet inversion. During inversion and in response to caffeine, some (but not all) cells transiently acquired a "bottle cell" morphology with a narrow apex and a bulbous base (fig. S9), reminiscent of animal

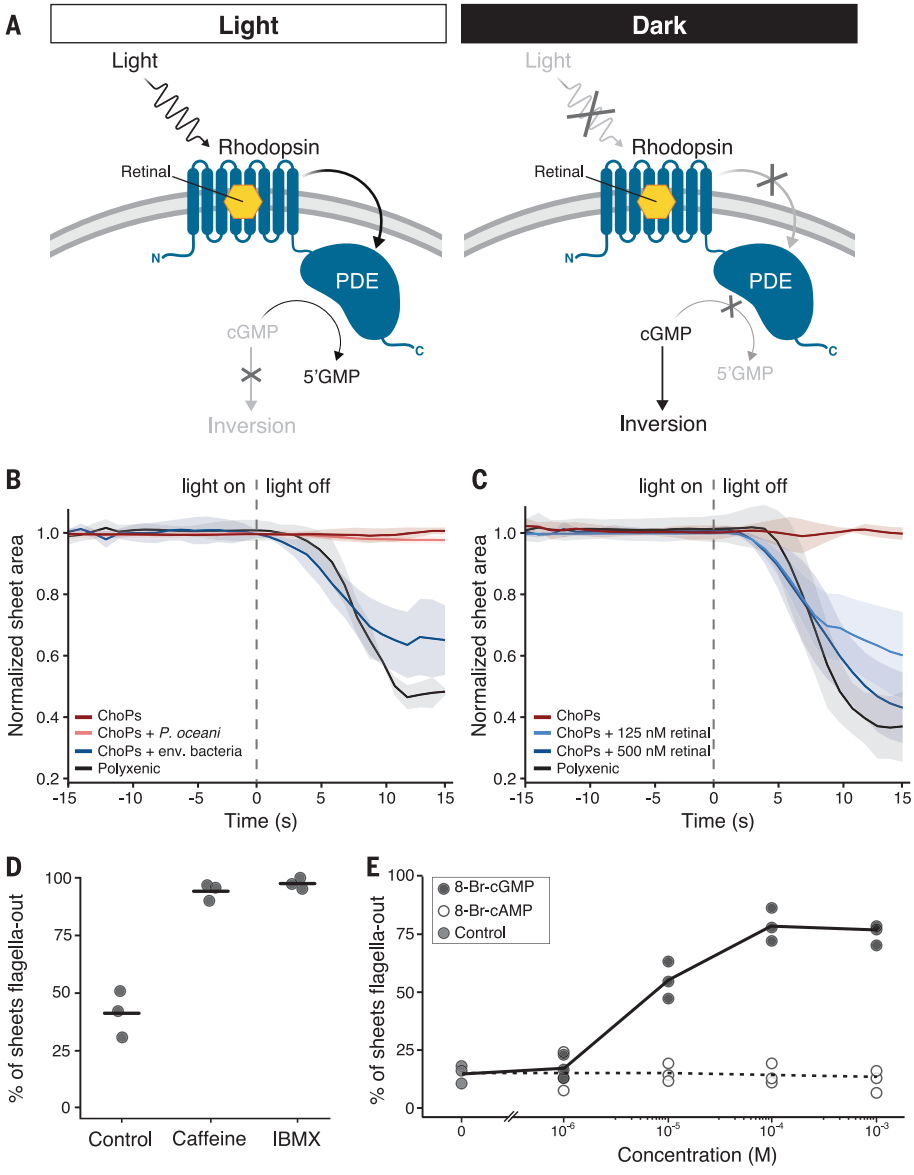

Fig. 3. *C. flexa* cells transduce light stimuli through a rhodopsin-cGMP pathway using bacterial carotenoids. (**A**) RhoPDE (blue), a choanoflagellate-specific enzyme rhodopsin. *C. flexa* encodes four copies of RhoPDE (fig. S2), each comprising an 8-transmembrane–pass type I (bacterial) rhodopsin fused to a cyclic nucleotide PDE. Photodetection by rhodopsin requires binding of the chromophore retinal. Under illumination (left panel), the rhodopsin domain activates the PDE domain, which hydrolyzes cGMP to 5′GMP, thereby reducing cellular cGMP levels. Upon light reduction (right panel), the PDE domain is inactivated, allowing cellular cGMP levels to rise. (**B**) A bacterial factor is required for light-regulated sheet inversion. In the presence of diverse "polyxenic" bacteria, *C. flexa* sheets inverted to flagella-out in response to decreased illumination (n = 3 colonies). By contrast, *C. flexa* sheets grown only with the bacterium *P. oceani* (ChoPs culture, n = 4 colonies) did not respond to changes in illumination. The photic response of the ChoPs culture was restored by inoculating with environmental bacteria from the polyxenic culture (ChoPs + env. bacteria, n = 3 colonies) but not by inoculating with *P. oceani* bacteria (ChoPs + *P. oceani*, n = 3 colonies). (**C**) Retinal (or one of its carotenoid precursors) is the bacterial molecule required for the photic response. The photic response of the ChoPs culture, which normally does not respond to light stimuli (n = 4 colonies), was restored by treatment with 125 nM or 500 nM retinal (n = 5 colonies each). Thus, retinal is required for inversion in response to reduced illumination. For (B) and (C), photic response was quantified as for Fig. 2. (**D**) PDE activity suppresses sheet inversion in *C. flexa*. Treatment with the PDE inhibitors caffeine (10 mM) or IBMX (1 mM) caused *C. flexa* colonies to invert to the flagella-out orientation in the absence of a photic stimulus (n = 3 independent trials; N = 52, 55, and 38 sheets for controls; N = 23, 31, and 40 sheets for caffeine; N = 42, 37, and 27 sheets for IBMX). (**E**) cGMP induces sheet inversion. Treating the ChoPs culture with a cell-permeant cGMP analog (8-Br-cGMP) caused sheets to invert into the flagella-out orientation in a dose-dependent manner in the absence of a photic stimulus. Treating with 8-Br-cAMP had no effect.

cells undergoing pronounced apical constriction (*41*, *42*). Caffeine treatment also induced shortening of the longitudinal actin fibers (fig. S9, G to H), suggesting that fiber contraction pulls the collar toward the basal pole.

Using an antibody raised against *C. flexa* myosin II as well as five different commercial myosin II antibodies (Fig. 5, M to S, and fig. S10), we found that *C. flexa* cells contain myosin that overlaps in regions with the apical actin ring (Fig. 5, M to P, and fig. S10) and longitudinal fibers (Fig. 5, Q to S), consistent with the idea that the apical actin network is contractile. Inhibition of myosin II activity with blebbistatin (*43*) abolished ring constriction in caffeine-treated dissociated cells (fig. S11A) and prevented sheet inversion (Fig. 5T), as did inhibition of dynamic actin polymerization with latrunculin B (*44*) and inhibition of phosphorylation of the myosin regulatory light chain with ML-7 (*45*) (Fig. 5T). None of these drugs affected flagellar beating, consistent with them specifically targeting actomyosin. Although compaction is normally associated with inversion, drug treatment resulted in sheet compaction in the absence of inversion (fig. S11B), suggesting that a baseline level of tension is needed to maintain spacing between cells. Together, these results suggest that sheet inversion requires apical constriction of an actomyosin network at the base of the collar (Fig. 5U).

The ancestry of apical constriction

The discovery of sheet bending driven by apical constriction in a multicellular choanoflagellate has several potentially important evolutionary implications. Epithelial sheet bending is a fundamental mechanism underlying animal embryonic development (*36*, *46*, *47*), and multicellular contractility also plays a fundamental role in the behavior of adult animals by allowing fine-tuned body deformations (*48*). As both embryonic and adult tissue contractility are found in nearly all animal lineages, including sponges (*49*, *50*), ctenophores (*51*, *52*), placozoans (*53*), cnidarians (*41*, *54*), and bilaterians (*36*, *37*, *55*), both were likely present in the last common animal ancestor. By contrast, collective contractility and apical constriction were hitherto unknown in close relatives of animals, making their origin mysterious.

The existence of actomyosin-mediated apical constriction in *C. flexa* raises the possibility

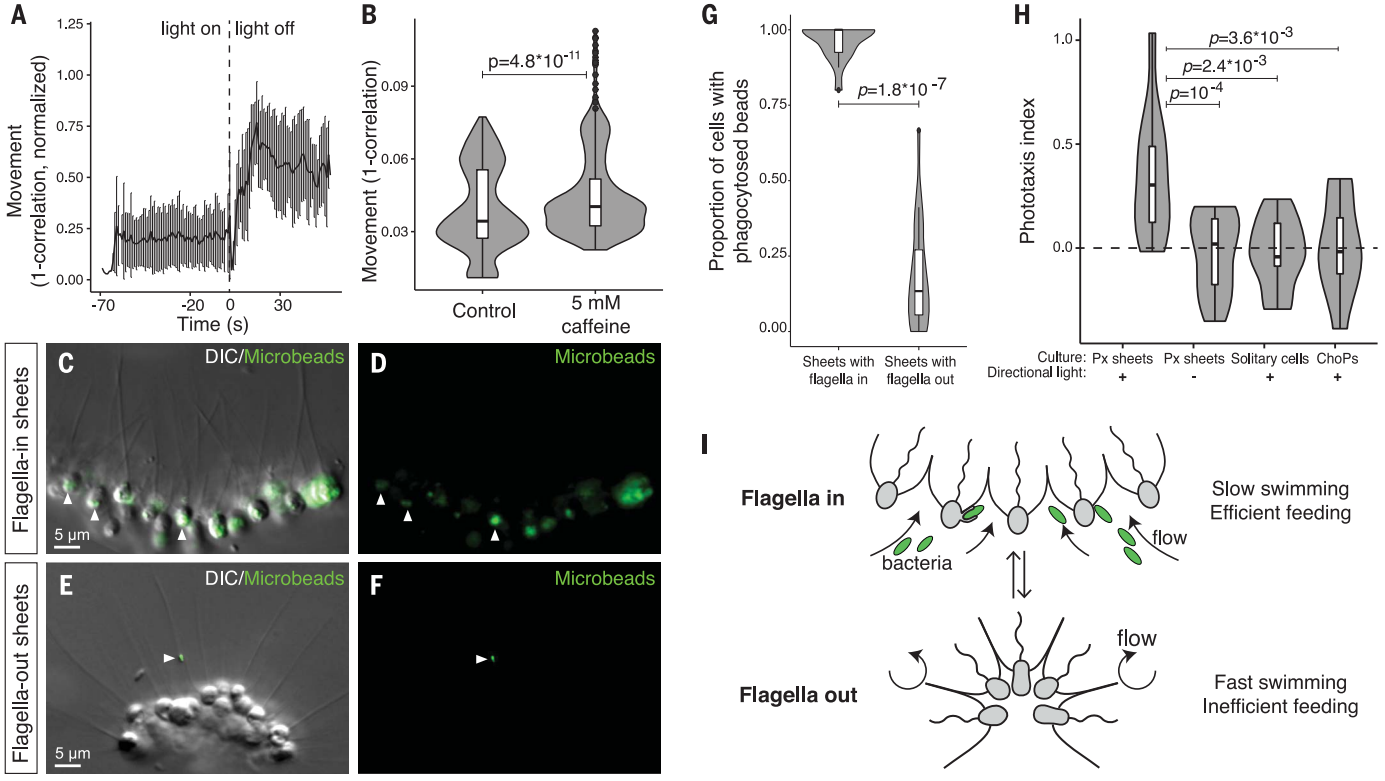

Fig. 4. Sheet inversion mediates a trade-off between swimming and feeding. (**A** and **B**) Flagella-out sheets swim faster than flagella-in sheets. (A) After light-to-dark–induced inversion, swimming speed increased quickly (movie S4), as quantified by an increase in the amount of movement (defined as 1-correlation, where "correlation" is the Pearson correlation between two consecutive frames). Movement was normalized between 0 and 1 for each of n = 9 movies. Gray shading: error bars representing standard deviation. (B) Sheets swim faster after caffeine-induced inversion under constant light. Movement quantified as in (A). n = 9 time-lapse movies for controls (relaxed sheet populations under constant light) and n = 10 movies for caffeine-treated samples. (**C** to **G**) Flagella-in sheets feed more efficiently than flagella-out sheets. Internalization of 0.2-µm fluorescent beads was used to quantify phagocytic activity. (C to F) Detection of fluorescent microbeads phagocytosed by flagella-in sheets (untreated) and flagella-out sheets (caffeine-treated), fixed after 1 hour. *C. flexa* cells were visualized by DIC (C and E) and beads by green fluorescence (C to F). Arrowheads: fluorescent beads [inside the cells in (C); stuck to a flagellum in (E)]. (G) Proportion of cells having phagocytosed beads in n = 17 flagella-in sheets compared with n = 21 flagella-out sheets. P value: χ^2 test. (**H**) *C. flexa* phototaxes in a retinal- and multicellularity-dependent manner, as measured by the phototaxis index, which quantifies directional accumulation of the sheets toward a localized light source (materials and methods). Light-responsive polyxenic (Px) sheets migrated toward a lateral light source over 1 hour (n = 12 experiments). By contrast, no directional accumulation was observed in Px sheets without directional light (n = 12 experiments), in dissociated single cells (n = 9 experiments), or in retinal-deprived light-insensitive monoxenic cultures (ChoPs; n = 10 experiments) that do not undergo inversion. P values: analysis of variance with Dunnett's correction. (**I**) In flagella-in sheets, flagellar beating generates a feeding flow that carries bacteria toward the basal side of the cells (fig. S7), allowing phagocytosis. In flagella-out sheets, flagellar beating causes rapid swimming, whereas the basal side of the cells faces inward, preventing prey capture.

that this cellular module might have been present in the last common ancestor of choanoflagellates and animals [which together compose the choanozoans (*1*)]. In addition to *C. flexa*, in which collar contractions occur in sheets (Fig. 5G), dissociated cells from sheets (Fig. 5, D and E), and naturally solitary "thecate" cells (movie S8), collar contractions have also been reported in unicellular stages from three other choanoflagellates: *Codosiga pulcherrima* (*56*), *Monosiga gracilis* (*57*), and *C. perplexa* (*7*). We found that four other choanoflagellate species, *Monosiga brevicollis*, *S. rosetta*, *Salpingoeca urceolata*, and *Diaphanoeca grandis*, which together cover both main branches of the choanoflagellate phylogenetic tree (*17*), display spontaneous changes in collar geometry occurring at the scale of a few seconds. *S. urceolata* (movie S9) and *M. brevicollis* (movie S10) showed spontaneous and reversible opening and closing of the collar (similar to *C. flexa*),

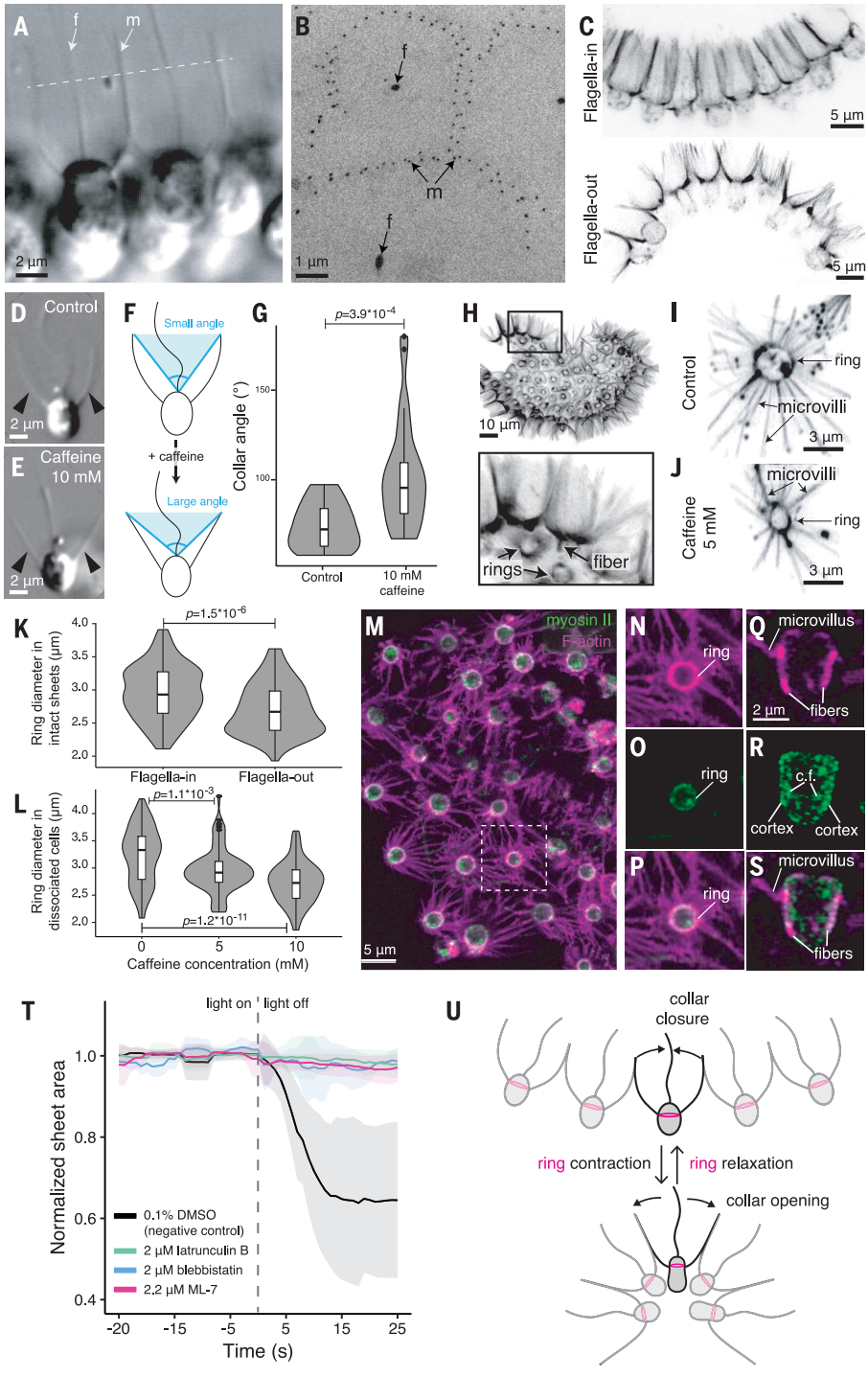

Fig. 5. Sheet inversion requires apical actomyosin cell contraction. (**A** and **B**) Cells in a sheet are linked by their collars. (A) DIC micrograph showing direct collar contacts between neighboring cells. f, flagellum; m, microvilli. Dotted line: approximate plane of section in (B). (B) Transmission electron micrograph of a transverse section through the collars of neighboring cells. (**C**) Collar morphology differs between flagella-in sheets (top) and flagella-out sheets (bottom). Cells in flagella-in sheets have barrel-shaped collars, whereas cells in flagella-out sheets have flared, conical collars. Staining: phalloidin. (**D** to **G**) Caffeine treatment of dissociated cells causes the collar to flare. (D) In the absence of caffeine, the collar of a cell from a dissociated colony curves upward. (E) In the presence of 10 mM caffeine, the collar of a cell from a dissociated colony straightened and flared open. Arrowheads: microvilli. (F) Differences in collar morphology where quantified in control and caffeine-treated single cells by measuring the collar angle (defined by the tip of two opposite microvilli and the base of the flagellum) (fig. S9). (G) Collar angles in caffeine-treated cells (n = 28) are wider than in control cells (n = 16). P value from Mann-Whitney U test. (**H**) Actin ring connected to longitudinal fibers is present at the base of each collar. (Inset) Higher magnification showing actin rings and a longitudinal fiber. Staining: phalloidin. (**I** to **L**) Actin ring constricts during inversion in intact sheets and in response to caffeine in isolated cells. (I and J) Actin ring observed with phalloidin in an untreated cell (I) and in a cell treated with 5 mM caffeine (J). (K) Ring diameter is larger in flagella-in sheets (n = 8 sheets, N = 124 cells) than in flagella-out sheets (n = 7 sheets, N = 110 cells). P value from Mann-Whitney U test. (L) Ring diameter is smaller in 10 mM caffeine-treated dissociated cells (n = 74) and 5 mM caffeine-treated dissociated cells (n = 82) than in untreated dissociated cells (n = 89). P values are from Dunnett's test for comparing several treatments with a control. (**M** to **S**) *C. flexa* myosin II localizes to the actin ring and longitudinal fibers. (M) Immunostained sheet showing apical rings of actin and myosin II at the apical poles of all cells. (N to P) Closer views showing the apical ring. (Q to S) Side view of a stained *C. flexa* cell (apical side up) showing cytoplasmic foci of myosin II (c.f.), as well as cortical staining (cortex) that overlaps with the longitudinal fibers. Green: anti-*C. flexa* myosin II antibody, magenta: rhodamine-phalloidin (fig. S10). (**T**) Treatment with inhibitors of actin polymerization (latrunculin B, n = 6), myosin contractility (blebbistatin, n = 6), or myosin activation by phosphorylation (ML-7, n = 9) prevented sheet inversion in response to light-to-dark transitions. n = 13 DMSO-treated controls. Photic response is quantified as in Fig. 2. DMSO, dimethyl sulfoxide. (**U**) Proposed role of actomyosin contractility in inversion.

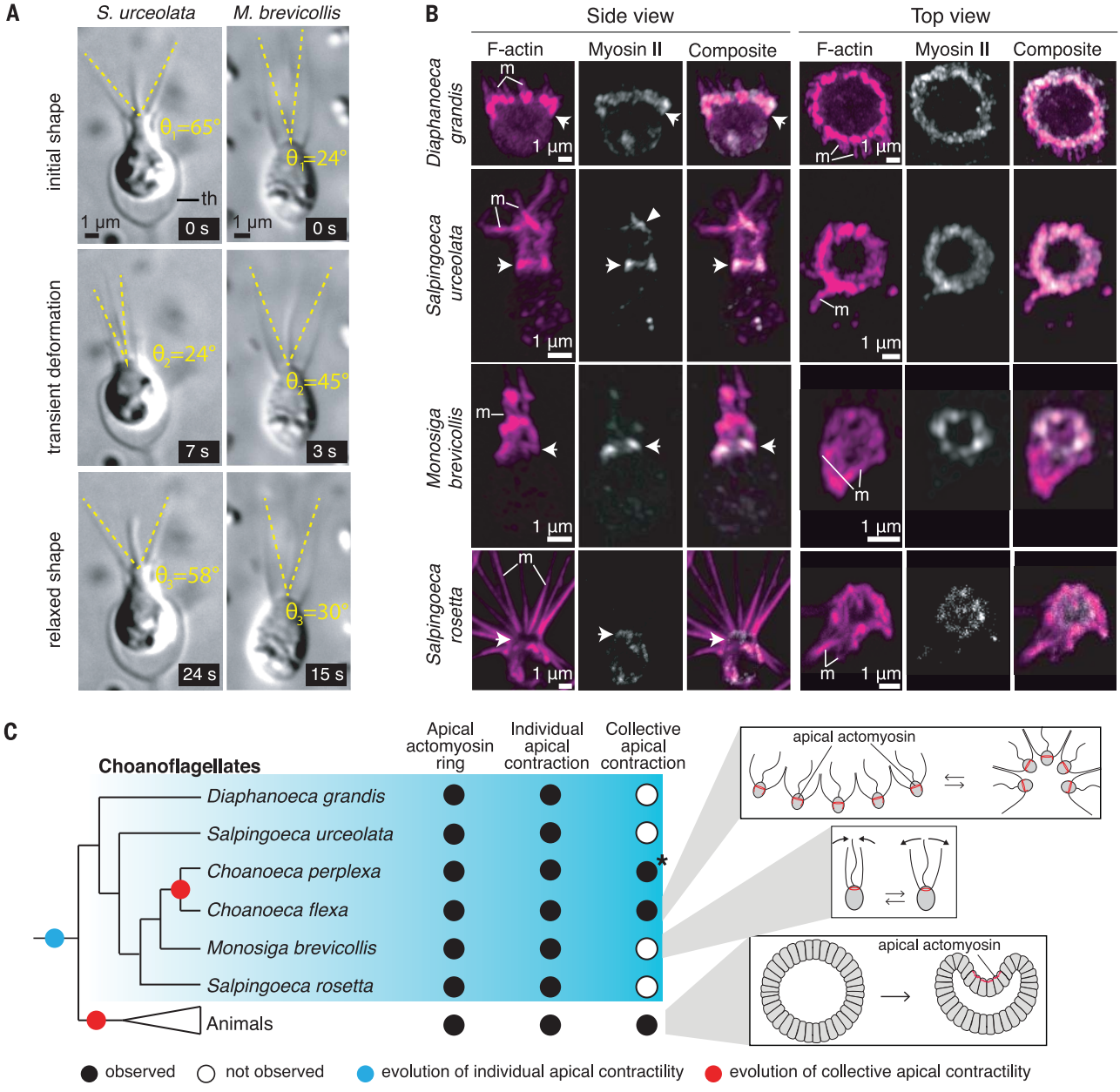

Fig. 6. Apical constriction is conserved in choanoflagellates. (**A**) Spontaneous collar contractions observed in *S. urceolata* and *M. brevicollis* (movies S8 and S9). Collar angles measured as in Fig. 5F. th, theca. (**B**) Apical actomyosin ring (arrows) is detected at the base of the collar in four representative choanoflagellate species. Myosin II was also detected in microvilli (m) in *S. urceolata* (arrowhead). (**C**) Apical constriction of individual cells was present in the last common ancestor of choanozoans and independently gave rise to multicellular apical constriction in *C. flexa* and in animals. **C. perplexa* was previously reported (*7*) to undergo transient inversions of colony curvature. On the basis of our study of *C. flexa*, we hypothesize that these inversions reflect collective apical constriction.

whereas *S. rosetta* (movie S11) and *D. grandis* (movie S12) displayed subtler shape changes (reorientation of individual microvilli and modulation of collar curvature, respectively) (Fig. 6A and fig. S12). Like animal epithelial cells and *C. flexa*, all four species have an apical actomyosin ring at the base of the collar (Fig. 6B). This suggests that the apical actomyosin ring is a conserved feature of choanoflagellate biology (Fig. 6C) and that unicellular apical constriction was present in the last common ancestor of choanoflagellates and animals.

What is the function of apical constriction in single cells? In some sessile choanoflagellates, including in the thecate form of *C. perplexa*, collar contraction in response to mechanical stimulation allows retraction of the cell inside an extracellular structure called a theca (*19*), suggesting it represents a defensive withdrawal reflex from predators or other threats. In free-swimming cells, collar contraction might fine-tune the hydrodynamics of swimming or feeding. For example, a closed collar might reduce drag and facilitate locomotion, whereas a flared collar could slow down swimming and increase collar area, thereby facilitating prey capture. Validation of these functional hypotheses will require direct testing.

In contrast to single-cell apical constriction, the multicellular sheet bending observed in *C. flexa* and *C. perplexa* (*7*) has not been reported in other choanoflagellates. This suggests that apical constriction was present in solitary cells in the last choanozoan common ancestor and was independently converted into multicellular sheet bending through the

evolution of intercellular junctions in animals (*58*) and the evolution of microvillar adhesions in *C. flexa*. Multicellular inversion has been proposed to have been part of the developmental repertoire of ancient animals (*1*, *59*), on the basis of the existence of whole-embryo inversion (from flagella-in to flagella-out) during calcareous sponge development (*60*). A similar inversion (but much slower, about an hour long, and irreversible) takes place during the development of the alga *Volvox* (*61*). Given the large evolutionary distance between choanoflagellates and volvocalean green algae, along with the absence of inversion in intervening branches, inversion likely evolved independently in both groups (*1*).

These observations suggest that apical actomyosin-mediated cell constriction evolved on the choanozoan stem lineage (Fig. 6B). Could polarized actomyosin contractility be even more ancient? Polarized actomyosin contractions have been implicated in multicellular morphogenesis in the fruiting body of the slime mold *Dictyostelium* (*62*) and may be homologous to those observed in choanoflagellates and animals. However, the absence of comparable processes in the intermediate branches between *Dictyostelium* and choanozoans raises the possibility that polarized cell contractions in *Dictyostelium* and apical constriction in choanozoans evolved independently (*63*). The ichthyosporean *Sphaeroforma arctica*, a close relative of choanozoans, forms large multinucleated spores that partition into distinct cells in an actomyosin-dependent process (*64*), providing an independent example of actomyosin-dependent multicellular development.

In animals, the control of multicellular contractions invariably relies either on the cooperation of multiple cell types [as in adult organisms (*54*, *55*, *65*)] or on complex programmed signaling cascades [as in embryos (*36*, *46*, *47*, *66*, *67*)]. By contrast, *C. flexa* directly converts sensory stimuli into collective contractions, without observable spatial cell differentiation, and evokes some hypotheses of early animal evolution that envisioned the first contractile tissues as homogeneous myoepithelia of multifunctional sensory-contractile cells (*68*).

The fact that contractility in *C. flexa* can be controlled by light represents another intriguing parallel to animal biology. Indeed, rhodopsin-cGMP pathways similar to that in *C. flexa* also underlie phototransduction in some animal cells [for example, bilaterian ciliary photoreceptors (*31*, *69*) and cnidarian photoreceptors (*70*, *71*)], as well as in fungal zoospores (*72*). In contrast with choanoflagellates, however, phototransduction in animal photoreceptors relies on a type II (eukaryotic) rhodopsin that activates a separate PDE through a G-protein intermediary (*31*, *69*) (fig. S13). Meanwhile, fungal zoospores use a distinct rhodopsin fusion protein (a type I rhodopsin fused to a guanylyl cyclase) to increase cellular cGMP in response to light (*72*) (fig. S13). If a RhoPDE fusion protein controls *C. flexa* phototransduction, this would represent a third independent solution to the problem of transducing information from a change in illumination into a change in cyclic nucleotide signaling.

Much remains to be discovered concerning the ecological function, mechanical underpinnings, and molecular mechanisms of phototransduction and apical constriction in *C. flexa*. A deeper understanding will require the development of molecular genetic tools, which have only recently been established in *S. rosetta* (*35*, *73*) and *D. grandis* (*74*). Nonetheless, *C. flexa* demonstrates how the exploration of choanoflagellate diversity can reveal biological phenomena and provides an experimentally tractable model for studying multicellular sensory-contractile coupling.

REFERENCES AND NOTES

1. T. Brunet, N. King, *Dev. Cell* **43**, 124–140 (2017).
2. A. Sebé-Pedrós, B. M. Degnan, I. Ruiz-Trillo, *Nat. Rev. Genet.* **18**, 498–512 (2017).
3. B. S. C. Leadbeater, *The Choanoflagellates* (Cambridge University Press, 2015).
4. N. King *et al.*, *Nature* **451**, 783–788 (2008).
5. I. Ruiz-Trillo, A. J. Roger, G. Burger, M. W. Gray, B. F. Lang, *Mol. Biol. Evol.* **25**, 664–672 (2008).
6. M. J. Dayel *et al.*, *Dev. Biol.* **357**, 73–82 (2011).
7. B. S. C. Leadbeater, *J. Mar. Biol. Assoc. U. K.* **63**, 135–160 (1983).
8. D. Laundon, B. T. Larson, K. McDonald, N. King, P. Burkhardt, *PLOS Biol.* **17**, e3000226 (2019).
9. D. J. Richter, P. Fozouni, M. B. Eisen, N. King, *eLife* **7**, e34226 (2018).
10. T. C. Levin, A. J. Greaney, L. Wetzel, N. King, *eLife* **3**, e04070 (2014).
11. N. King, C. T. Hittinger, S. B. Carroll, *Science* **301**, 361–363 (2003).
12. M. Abedin, N. King, *Science* **319**, 946–948 (2008).
13. G. L. Miño, M. A. R. Koehl, N. King, R. Stocker, *Limnol. Oceanogr. Lett.* **2**, 37–46 (2017).
14. J. B. Kirkegaard, A. Bouillant, A. O. Marron, K. C. Leptos, R. E. Goldstein, *eLife* **5**, e18109 (2016).
15. R. A. Alegado *et al.*, *eLife* **1**, e00013 (2012).
16. A. Woznica, J. P. Gerdt, R. E. Hulett, J. Clardy, N. King, *Cell* **170**, 1175–1183.e11 (2017).
17. M. Carr *et al.*, *Mol. Phylogenet. Evol.* **107**, 166–178 (2017).
18. C. Nielsen, *Animal Evolution: Interrelationships of the Living Phyla* (Oxford Univ. Press, ed. 3rd, 2012).
19. B. S. C. Leadbeater, *J. Mar. Biol. Assoc. U. K.* **57**, 285–301 (1977).
20. G. Jékely, Evolution of phototaxis. *Philos. Trans. R. Soc. B Biol. Sci.* **364** (2009),
21. M. Watari *et al.*, *J. Biol. Chem.* **294**, 3432–3443 (2019).
22. K. Yoshida, S. P. Tsunoda, L. S. Brown, H. Kandori, *J. Biol. Chem.* **292**, 7531–7541 (2017).
23. L. B. Lamarche *et al.*, *Biochemistry* **56**, 5812–5822 (2017).
24. Y. Tian, S. Gao, S. Yang, G. Nagel, *Biochem. J.* **475**, 1121–1128 (2018).
25. J. L. Spudich, *Trends Microbiol.* **14**, 480–487 (2006).
26. T. Brunet, B. T. Larson, T. A. Linden, N. King, Choanoeca flexa transcriptome and predicted nonredundant proteome, Figshare, Version 2 (2019); doi: 10.6084/m9.figshare.8216291.
27. I. Chaves *et al.*, *Annu. Rev. Plant Biol.* **62**, 335–364 (2011).
28. A. Coulon, C. C. Chow, R. H. Singer, D. R. Larson, *Nat. Rev. Genet.* **14**, 572–584 (2013).
29. J. E. Pérez-Ortín, P. M. Alepuz, J. Moreno, *Trends Genet.* **23**, 250–257 (2007).
30. O. P. Ernst *et al.*, *Chem. Rev.* **114**, 126–163 (2014).
31. D. Arendt, *Int. J. Dev. Biol.* **47**, 563–571 (2003).
32. E. García-Valdés, M. Gomila, M. Mulet, J. Lalucat, *Genome Announc.* **6**, e00254–e18 (2018).
33. V. Boswell-Smith, D. Spina, C. P. Page, *Br. J. Pharmacol.* **147** (Suppl 1), S252–S257 (2006).
34. R. E. Weishaar, M. H. Cain, J. A. Bristol, *J. Med. Chem.* **28**, 537–545 (1985).
35. L. A. Wetzel *et al.*, *eLife* **7**, e41482 (2018).
36. A. C. Martin, B. Goldstein, *Development* **141**, 1987–1998 (2014).
37. J. M. Sawyer *et al.*, *Dev. Biol.* **341**, 5–19 (2010).
38. T. A. Richards, T. Cavalier-Smith, *Nature* **436**, 1113–1118 (2005).
39. A. Sebé-Pedrós, X. Grau-Bové, T. A. Richards, I. Ruiz-Trillo, *Genome Biol. Evol.* **6**, 290–305 (2014).
40. D. J. Richter, N. King, *Annu. Rev. Genet.* **47**, 509–537 (2013).
41. C. R. Magie, M. Daly, M. Q. Martindale, *Dev. Biol.* **305**, 483–497 (2007).
42. J. Y. Lee, R. M. Harland, *Dev. Biol.* **311**, 40–52 (2007).
43. M. Kovács, J. Tóth, C. Hetényi, A. Málnási-Csizmadia, J. R. Sellers, *J. Biol. Chem.* **279**, 35557–35563 (2004).
44. T. Wakatsuki, B. Schwab, N. C. Thompson, E. L. Elson, *J. Cell Sci.* **114**, 1025–1036 (2001).
45. M. Saitoh, T. Ishikawa, S. Matsushima, M. Naka, H. Hidaka, *J. Biol. Chem.* **262**, 7796–7801 (1987).
46. C. P. Heisenberg, Y. Bellaïche, *Cell* **153**, 948–962 (2013).
47. D. Gilmour, M. Rembold, M. Leptin, *Nature* **541**, 311–320 (2017).
48. E. N. Marieb, K. Hoehn, *Human Anatomy & Physiology* (Pearson, 2015).
49. M. Nickel, C. Scheer, J. U. Hammel, J. Herzen, F. Beckmann, *J. Exp. Biol.* **214**, 1692–1698 (2011).
50. S. P. Leys, D. Eerkes-Medrano, *Integr. Comp. Biol.* **45**, 342–351 (2005).
51. C. Dayraud *et al.*, *BMC Evol. Biol.* **12**, 107 (2012).
52. K. Pang, M. Q. Martindale, *Dev. Genes Evol.* **218**, 307–319 (2008).
53. S. Armon, M. S. Bull, A. Aranda-Diaz, M. Prakash, *Proc. Natl. Acad. Sci. U.S.A.* **115**, E10333–E10341 (2018).
54. P. R. H. Steinmetz *et al.*, *Nature* **487**, 231–234 (2012).
55. T. Brunet *et al.*, *eLife* **5**, e19607 (2016).
56. H. James-Clark, *Mem. Bost. Soc. Nat. Hist.* **1**, 305–340 (1867).
57. W. S. Kent, *Ann. Mag. Nat. Hist.* **5**, 1–17 (1878).
58. S. A. Nichols, B. W. Roberts, D. J. Richter, S. R. Fairclough, N. King, *Proc. Natl. Acad. Sci. U.S.A.* **109**, 13046–13051 (2012).
59. D. Arendt, E. Benito-Gutierrez, T. Brunet, H. Marlow, *Philos. Trans. R. Soc. B Biol. Sci.* **370**, 20150286 (2015).
60. W. Franzen, *Zoomorphology* **107**, 349–357 (1988).
61. S. Höhn, A. R. Honerkamp-Smith, P. A. Haas, P. K. Trong, R. E. Goldstein, *Phys. Rev. Lett.* **114**, 178101 (2015).
62. D. J. Dickinson, D. N. Robinson, W. J. Nelson, W. I. Weis, *Dev. Cell* **23**, 533–546 (2012).
63. D. J. Dickinson, W. J. Nelson, W. I. Weis, *BioEssays* **34**, 833–840 (2012).
64. O. Dudin *et al.*, *bioRxiv* 10.1101/563726 (2019).
65. F. Varoqueaux *et al.*, *Curr. Biol.* **28**, 3495–3501.e2 (2018).
66. T. Merle, E. Farge, *Curr. Opin. Cell Biol.* **55**, 111–118 (2018); 10.1016/j.ceb.2018.07.003.
67. A. Bailles *et al.*, *bioRxiv* **430512** (2019); https://doi.org/10.1101/430512.
68. G. O. Mackie, *Q. Rev. Biol.* **45**, 319–332 (1970).
69. X. Zhang, R. H. Cote, *Front. Biosci.* **10**, 1191–1204 (2005).
70. M. Koyanagi *et al.*, *Proc. Natl. Acad. Sci. U.S.A.* **105**, 15576–15580 (2008).
71. D. C. Plachetzki, C. R. Fong, T. H. Oakley, *Proc. Biol. Sci.* **277**, 1963–1969 (2010).
72. G. M. Avelar *et al.*, *Curr. Biol.* **24**, 1234–1240 (2014).
73. D. S. Booth, H. Szmidt-Middleton, N. King, *Mol. Biol. Cell* **29**, 3026–3038 (2018).
74. R. Li, I. Neundorf, F. Nitsche, *bioRxiv* **260190** (2018); https://doi.org/10.1101/260190.

ACKNOWLEDGMENTS

We thank the Canadian Institute for Advanced Research for support of field work in Curaçao, P. Keeling for access to the microscope used for Fig. 1C, the staff and students of the 2018 MBL Physiology course, Zeiss for access to an AxioZoom, T. Gerbich and T. Fadero for advice on early phototaxis experiments, D. Jorgens and G. Min (from the UC Berkeley Electron Microscopy Laboratory) for help with SEM, M. Coyle and C. Erikson for advice on transcriptome assembly, M. Sigg and the UC Berkeley Functional Genomic Laboratory for help with iTag sequencing, and D. Bilder, M. Feller, B. Goldstein, and K. Scott for critical feedback on the manuscript. **Funding:** T.A.L. and B.T.L. were supported by NSF GRP Fellowships (B.T.L.: DGE 1106400). T.A.L. was supported by the Berkeley Fellowship for Graduate Study. T.B. was supported by the EMBO long-term fellowship (ALTF 1474-2016) and by the Human Frontier Science Program long-term fellowship (000053/2017-L). **Author contributions:** T.B., B.T.L., and T.A.L.: conceptualization, investigation, methodology, formal analysis, visualization, writing. M.J.A.V.: project administration and resources. K.M.: investigation and visualization. N.K.: conceptualization,

supervision, project administration, and writing. **Competing interests:** The authors declare no competing interests. **Data and materials availability:** The name-bearing hapantotype of *C. flexa* is deposited with the California Academy of Sciences Invertebrate Zoology Collections (San Francisco) with accession number CASIZ 197968. Raw RNAseq reads used to assemble the *C. flexa* transcriptome have been deposited at the NCBI SRA (accession number/BioProject PRJNA540068, BioSample SAMN11533889). Transcriptome and predicted nonredundant proteome are available on Figshare (*26*). mRNA sequences and predicted amino acid sequences for genes of interest are deposited at GenBank: myosin regulatory light chain (MK787241), myosin heavy chain (MK787240), and the four RhoPDEs (MN013138, MN013139, MN013140, and MN013141).

SUPPLEMENTARY MATERIALS

science.sciencemag.org/content/366/6463/326/suppl/DC1
Materials and Methods
Figs. S1 to S14
Tables S1 to S4
References (*75*–*94*)
Movies S1 to S14

View/request a protocol for this paper from *Bio-protocol*.

6 June 2019; accepted 16 September 2019
10.1126/science.aay2346

Science

Light-regulated collective contractility in a multicellular choanoflagellate

Thibaut Brunet, Ben T. Larson, Tess A. Linden, Mark J. A. Vermeij, Kent McDonald and Nicole King

Science **366** (6463), 326-334.
DOI: 10.1126/science.aay2346

Origins of collective contraction

In contrast to plants and fungi, animals can deform their bodies by the collective activity of contractile cells. Collective contractility underlies processes such as gastrulation and muscle-based motility. Brunet *et al.* report that a close relative of animals, a choanoflagellate they name *Choanoeca flexa*, forms cup-shaped colonies that undergo collective contractility, leading to a rapid change in colony morphology (see the Perspective by Tomancak). *C. flexa* colonies are each composed of a monolayer of polarized cells. In response to sudden darkness, a light-sensing protein triggers coordinated, polarized contraction of *C. flexa* cells, which results in colony inversion. The cellular mechanisms underlying this process are conserved between *C. flexa* and animals, indicating that their last common ancestor was also capable of polarized cell contraction.

Science, this issue p. 326; see also p. 300

Science (print ISSN 0036-8075; online ISSN 1095-9203) is published by the American Association for the Advancement of Science, 1200 New York Avenue NW, Washington, DC 20005. The title *Science* is a registered trademark of AAAS.